Neuroradiology (2015) 57:155–162
DOI 10.1007/s00234-014-1447-7

DIAGNOSTIC NEURORADIOLOGY

Potential of 80-kV high-resolution cone-beam CT imaging combined with an optimized protocol for neurological surgery

Seisaku Kanayama · Takayuki Hara · Yusuke Hamada · Yuji Matsumaru

Received: 15 July 2014 / Accepted: 28 September 2014 / Published online: 5 November 2014

Abstract
Introduction With the development of computed tomography (CT) and magnetic resonance imaging (MRI), the use of conventional X-ray angiography including digital subtraction angiography (DSA) for diagnosis has decreased, as it is an invasive technique with a risk of neurological complications. However, X-ray angiography imaging technologies have progressed markedly, along with the development of endovascular treatments. A newly developed angiography technique using cone-beam CT (CBCT) technology provides higher spatial resolution than conventional CT. Herein, we describe the potential of this technology for neurosurgical operations with reference to clinical cases.
Methods Two hundred twenty-five patients who received 80-kV high-resolution CBCT from July 2011 to June 2014 for preoperative examinations were included in this study. For pathognomonical cases, images were taken with suitable reconstruction modes and contrast protocols. Cases were compared with intraoperative findings or images from other modalities.
Results We observed the following pathognomonical types: (1) imaging of the distal dural ring (DDR) and the surrounding structure for paraclinoid aneurysms, (2) imaging of thin blood vessels, and (3) imaging of both brain tumors and their surrounding anatomy. Our devised 80-kV high-resolution CBCT imaging system provided clear visualization of detailed anatomy when compared with other modalities in almost all cases. Only two cases provided poor visualization due to movement artifact.
Conclusion Eighty-kilovolt high-resolution CBCT has the potential to provide detailed anatomy for neurosurgical operations when utilizing suitable modes and contrast protocols.

Keywords 80-kV cone-beam CT · XperCT · Vaso CT

Abbreviations

CT	Computerized tomography
CTA	Computed tomography angiography
MRI	Magnetic resonance imaging
MRA	Magnetic resonance angiography
DSA	Digital subtraction angiography
CBCT	Cone-beam CT
DDR	Distal dural ring

Introduction

Diagnostic imaging technology has rapidly advanced with the development of multi-detector computed tomography (CT) and high-field magnetic resonance imaging (MRI) [1–4]. Although the use of X-ray angiography including digital subtraction angiography (DSA) for diagnosis is reducing due to these technologies, its combination with novel devices for percutaneous intervention in the field of endovascular treatment holds great potential. Recently, rotational angiography combined with cone-beam CT (CBCT) has provided marked advances in the imaging of low contrast anatomy such as soft tissue. For example, CBCT of low kilovolts for higher contrast can extract maximum spatial resolution from the latest flat-panel detector on X-ray angiography [5–7]. Thus, the aim of our study was to use 80-kV high-resolution CBCT for

S. Kanayama (✉) · T. Hara
Department of Neurosurgery, Toranomon Hospital, 2-2-2 Minatoku Toranomon, Tokyo 105-8470, Japan
e-mail: skanayama-nsu@umin.ac.jp

Y. Hamada
Department of Radiology, Toranomon Hospital, Tokyo, Japan

Y. Matsumaru
Department of Neuro-Endovascular Therapy, Toranomon Hospital, Tokyo, Japan

imaging in neurosurgical operations to determine suitable reconstruction modes and contrast protocols depending on pathognomonical types.

Materials and methods

We used the Allura Xper FD20/20 (Philips Healthcare, Best, the Netherlands) for X-ray angiography. The CBCT imaging system combined with a flat detector was termed XperCT (Philips Healthcare), and the acquisition protocols and post-processing algorithms were embedded in the system. Imaging with the XperCT system consisted of motorized rotational movement (propeller scan) of a C-arm in the plane perpendicular to the longitudinal table axis. The 80-kV high-resolution XperCT acquires 620 fluoroscopic frames in a circular motion at a frame rate of 30 frames/s, total rotation time of 20 s, an angle of 240° (±120°) with a rotation speed of 22°/s, using a 1,024×1,024 pixel matrix detector with an 8-in field of view and a low 80-kV tube voltage. The head of the patient was positioned at the isocenter of the system, and a propeller C-arm scan was applied. During the propeller acquisition movement, the dataset was transferred automatically via a real-time digital link to the 3D workstation (Xtravision; Philips Healthcare) for processing. The reconstructed 3D volume image, displayed in a 2,563-pixel matrix as a default reconstruction size, was available within 1 min. Different types of image post-processing (i.e., beam hardening and scatter corrections) were applied to achieve maximal spatial and contrast resolution qualities. We used two different modes in the reconstruction process: mode 1 for images that required higher spatial resolution and mode 2 for images that required higher contrast resolution. Additional reconstructions were performed with variable volume matrices or dimensions of reconstructed volume (512^3 spatial resolution matrix as a maximum). Mode 1 and mode 2 (commercially termed VasoCT; Philips Healthcare) provide different filtering for image processing. Once displayed on the 3D monitor, the reconstructed results could be rotated, zoomed, and panned and then displayed in different volume-rendering formats and display modes (multi-planar reconstruction [MPR] or single-slice view).

In the transarterial contrast injection, a 4F catheter was used via the femoral artery under local anesthesia. The catheter was brought to the targeted cervical segment through the internal carotid artery, external carotid artery, or the vertebral artery. The initial location of the C-arm and table was set to the center of the lesion. Contrast injection of a nonionic (370 mg I/ml) contrast material (Iopamiron370; Iopamidol, Bayer-Schering, Berlin, Germany) with two to three dilutions was performed by hand to obtain good contrast. The total volume of injected contrast material during the acquisition was 20–30 ml at a rate of 1 ml/s (Table 1).

Table 1 Imaging conditions

	3D-RA	80-kV HR XperCT
Tube voltage	80–90 kV	80 kV
Scan flame rate	30 frames/s	30 frames/s
Scan time	4.1 s	20 s
Inch size	6–9 in.	8 in.
Focus size	0.7 mm	0.4 mm
Injecting method	Injector	Hand injection
Injection speed	3–3.5 ml/s	1 ml/s
Dilution rate	Equal	2–3 times
Injection amount	25 ml	20–30 ml
Spatial resolution	–	Mode 1
Contrast resolution	–	Mode 2

RA rotational angiography, *HR* high resolution

For mode selection, mode 1 provided superior high-frequency spatial resolution and was applied to cases for intracranial stent visualization and lesion contacting with or surrounded by high X-ray absorption anatomy. Mode 2 provided superior contrast resolutions with lower noise and was applied to the vein visualization or visualization of thinner vessels such as perforators. 3D-rotation angiography imaging was performed in aneurism cases, while 3D-CTA and MRI imaging were performed for tumor cases. The images obtained using the 80-kV high-resolution XperCT were compared with other modalities, and in cases accompanied by open surgery, images were compared with surgical findings.

Number of patients

Two hundred twenty-five patients were included in the study (108 males, 117 females; 24–79 years old; mean 57.7 years). All patients were examined at our hospital between July 2011 and June 2014 for preoperative evaluation assessment of cerebrovascular disease (133 patients; 59.1 %) and brain tumor (92 patients; 40.9 %). We used 80-kV high-resolution XperCT with mode 1 in 36 cases, and 80-kV high-resolution XperCT with mode 2 for 200 cases.

Results

We performed cannulation of the intended blood vessel in all cases. No ischemic complications occurred during the procedures. Poor visualization of anatomy due to movement artifact was seen in two cases. Below, we describe the clinical images with objective evaluation from three pathognomonical types with six definitive cases of cerebrovascular surgery and brain tumor.

Imaging of the distal dural ring and the surrounding structure of the cavernous sinus for paraclinoid aneurysms

In our new imaging method using 80-kV HR XperCT with mode 1, we took advantage of the enhanced effect of the dura using contrast material to illustrate the enhanced contrast difference between the dura and the surrounding bony structure. In this procedure, three times diluted contrast was injected via the common carotid artery of the lesion side to obtain improved dura enhancement effects through the dura-feeding vessels. In the seven aneurism cases (three males, four females) in the carotid artery close to the dura, visualization of the DDR was attempted and objective testing of the images was performed by three physicians (two neurosurgeons and one physician for dedicated neuroendovascular treatment). As open surgery for clipping was performed in two cases out of seven, DDR images were also compared with surgical findings. Objective testing found good visualization of DDR in six cases and insufficient visualization of DDR in one case. The case of insufficient visualization was considered to be caused by unstable manual injection.

Case 1 A 47-year-old man with a left internal carotid artery (ICA)-ruptured paraclinoid aneurysm (Fig. 1a) was treated surgically. In 80-kV HR XperCT with mode 1, the tuberculum sellae, the anterior clinoid process, and the ophthalmic artery (anatomical landmarks surrounding the DDR) were shown together with the DDR itself (Fig. 1b–d). These landmarks agreed with the findings during surgery (Fig. 1e).

Imaging of thin blood vessels including the stream of the Sylvian vein and perforators

The 80-kV high-resolution XperCT with mode 2, which provides superior contrast characteristics in addition to higher spatial resolution, can depict thin blood vessels including perforators. XperCT scanning starting 10 s after the injection of two to three times diluted contrast media was able to visualize both arteries and veins.

Case 2 A 63-year-old woman with a right ICA unruptured aneurysm (Fig. 2a) was treated surgically by a trans-Sylvian approach. The surgical view could be reconstructed, and clear visualization of the vein and the connection of thin vessels of the vein (including the venous pathway consisting of a superficial Sylvian vein and the deep middle Sylvian vein) was observed. Thus, useful information on veins was obtained preoperatively.

Case 3 A 65-year-old man with a left middle cerebral artery (MCA) ruptured aneurysm was treated surgically by a trans-Sylvian approach. 3D rotational angiography (3D-RA) clearly showed the aneurysmal shape (Fig. 3a). The 80-kV high-resolution XperCT with mode 2 was inferior for visualization at the site of the anterior circulation because diluted contrast media was used. However, 80-kV high-resolution XperCT with mode 2 showed additional detailed information of the surrounding small vessels such as the veins and perforators (Fig. 3b). The effectiveness of 80-kV high-resolution XperCT with mode 2 for preoperative evaluations was even more

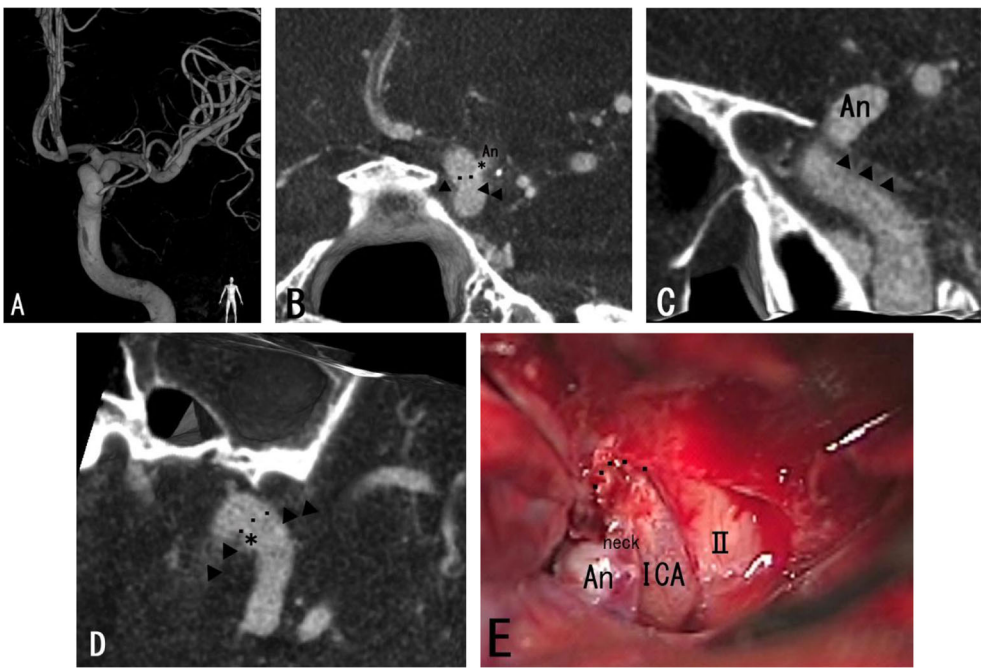

Fig. 1 **a** Left carotid 3D angiographic reconstruction (anteroposterior view) shows a left ICA aneurysm that arises from the C2 segment. **b–d** 80-kV high-resolution XperCT with mode 1 MPR images in the coronal, lateral, and operative views show the extradural paraclinoid aneurysm, projecting superiolaterally. The structures around the juxta-dural ring area are visible, indicating the DDR (*dotted line*) and the dura mater (*arrowhead*). The aneurysmal neck (*asterisk*) is located adjacent to the DDR. **e** Intraoperative view after removal of the anterior clinoid process and sectioning of the DDR (*dotted line*) confirming the accuracy of 80-kV high-resolution XperCT with mode 1 images. Second cranial nerve (*II*)

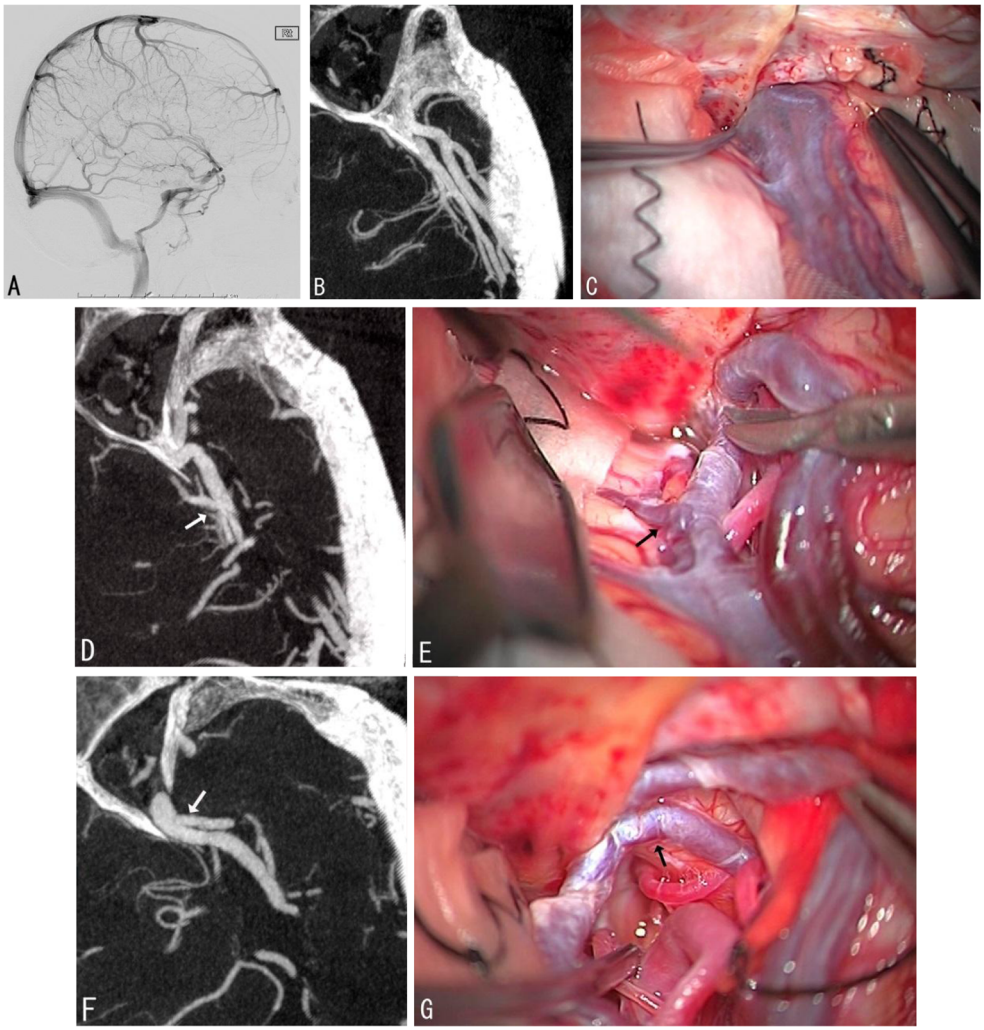

Fig. 2 **a** Right carotid angiogram (lateral view) at the venous phase shows several superficial Sylvian veins and a cavernous-type drainage that drains into the sphenoparietal and cavernous sinuses. **b**, **c** Operative view of 80-kV high-resolution XperCT with mode 2 (**b**) clearly shows two mainly superficial veins and is compatible with the intraoperative photograph (**c**). **d**, **e** Consecutive section of 80-kV high-resolution XperCT with mode 2 (**d**) shows a fronto-orbital vein (*arrow*) flowing into the fronto-Sylvian vein, which is an obstacle in dissecting via the frontal side but should be preserved, and is compatible with the intraoperative photograph (**e**). **f**, **g** Compared with the intraoperative photograph (**g**), a consecutive section of 80-kV high-resolution XperCT with mode 2 (**f**) can show the common vertical trunk of insular veins (*arrow*) flowing into the sphenoparietal sinus, which cannot be observed from the surface and is difficult to detect by other modalities

valuable in cases with poor visibility such as in aneurysmal surgery for a subarachnoid hemorrhage.

Case 4 A 63-year-old woman with a basilar apex unruptured aneurysm. 3D-RA (Fig. 4a) showed a poor contrast effect under the influence of the laminar flow and turbulent flow at the site of posterior circulation, whereas 80-kV high-resolution XperCT with mode 2 (Fig. 4b) provided clear visualization of perforators at a high spatial resolution and with a slow injection of contrast medium.

Imaging of a brain tumor and the surrounding anatomy

Detailed information on brain tumors and the surrounding anatomy could also be obtained using 80-kV high-resolution XperCT with mode 2 and 80-kV high-resolution XperCT with mode 1 properly.

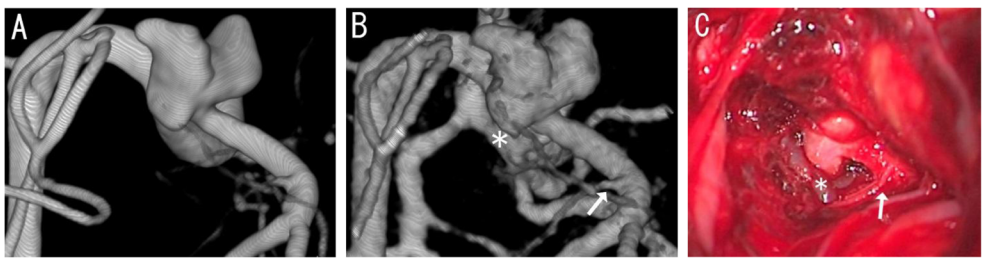

Fig. 3 **a** A 3D-RA showing the patient's middle cerebral artery aneurysm. **b** Eighty-kilovolt high-resolution XperCT with mode 2 volume rendering image shows a perforator (*arrow*) and vein (*asterisk*) surrounding the aneurysm, which cannot be detected by 3D-RA. **c** Intraoperative photographs similarly show the perforator (*arrow*) and vein (*asterisk*) covered by a thick hematoma

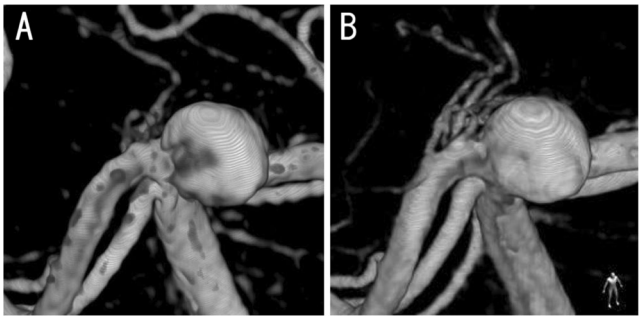

Fig. 4 **a** The 3D-RA following a left vertebral artery injection shows a basilar apex aneurysm but unequal concentration. **b** Eighty-kilovolt high-resolution XperCT with mode 2 volume rendering image shows equal concentrations and clear visualization of the perforators

Case 5 A 37-year-old man with a foramen magnum meningioma (Fig. 5a) with many feeders underwent a tumor resection. In such a brain tumor operation, hemostasis of feeders is important to control bleeding. The 80-kV high-resolution XperCT with mode 1 was able to simultaneously visualize the enhanced anatomy of the soft tissue, bones, and even vessels that run into bone in the focused lesion. Thus, the operator could confirm the point where a feeder flows into and the attached part of the tumor. This imaging is particularly useful in surgery for skull base tumors, which have many feeders and are surrounded by the complicated bony structure.

Case 6 A 59-year-old man with an olfactory groove meningioma (Fig. 6a–c) underwent a resection of the tumor. In Fig. 6d, 80-kV high-resolution XperCT with mode 2 image showed a small artery surrounding the tumor, which could not be seen on MRI or 3D-CT (Fig. 6b, c). With increased tumor growth, the surrounding vessels that must be preserved become involved in the tumor. In such cases, a preoperative evaluation using 80-kV high-resolution XperCT with mode 2 is useful as it provides a high-resolution compared with other modalities.

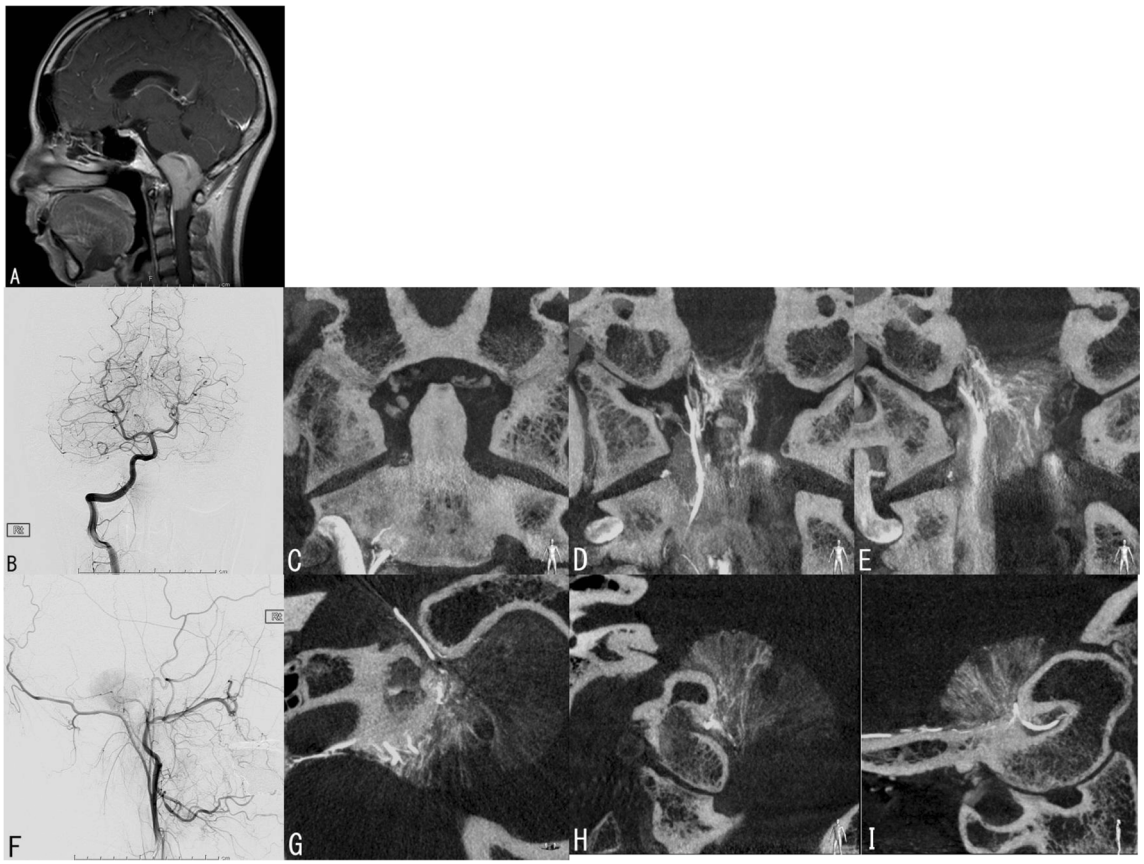

Fig. 5 **a** The sagittal T1-weighted MRI image with contrast shows a large mass located ventrolaterally in the foramen magnum. **b** Right vertebral angiogram (anteroposterior view) shows that the tumor stain is supplied by the anterior meningeal branch of the vertebral artery. **c**–**e** In 80-kV high-resolution XperCT with mode 1 coronal images (**c**, **d**), the feeder originates from the C3 portion of the vertebral artery, and this feeder supplies the lower part of the tumor (**e**). **f** Right external carotid angiogram (lateral view) shows that the tumor stain is supplied by the hypoglossal branch of the ascending pharyngeal artery. **g**–**i** Eighty-kilovolt high-resolution XperCT with mode 1 axial (**g**) and coronal (**h**) images show that the feeder is the hypoglossal branch of the ascending pharyngeal artery running through the hypoglossal canal and that this feeder supplies the upper part of the tumor (**h**)

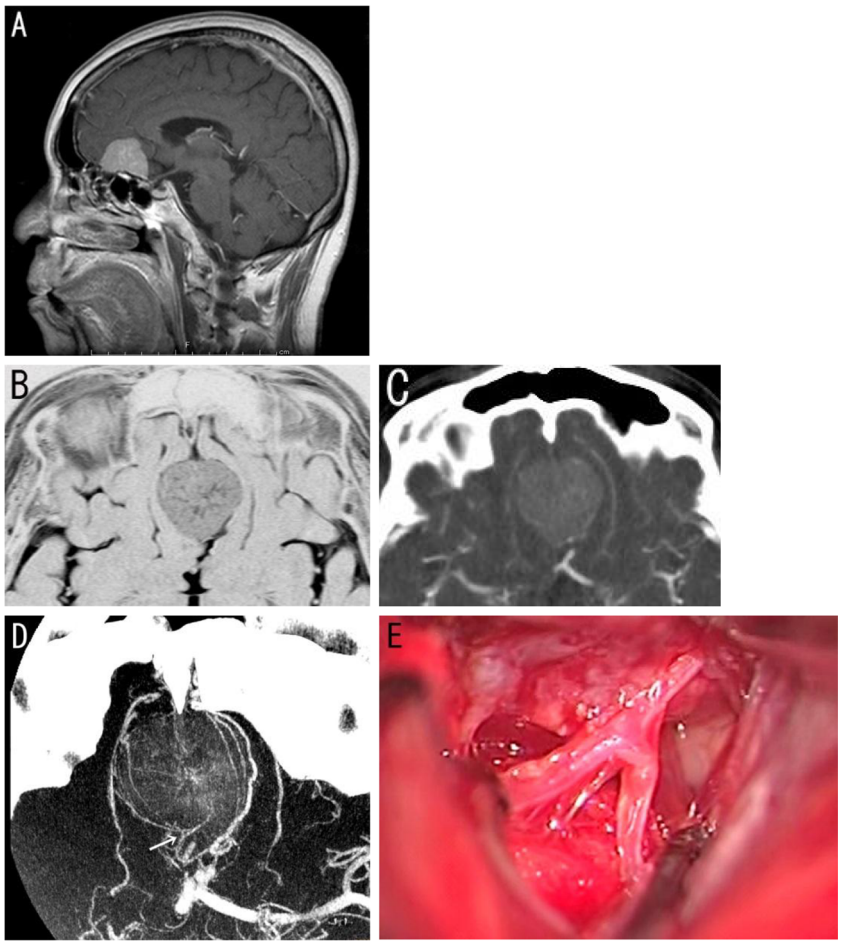

Fig. 6 **a** Sagittal T1-weighted MRI image with contrast showing a large mass located at the anterior skull base. **b**–**d** Eighty-kilovolt high-resolution XperCT with mode 2 image (**d**) shows that branches of the anterior cerebral artery surround the tumor (*arrow*) but cannot be detected by MRI cisternography (**b**) or multi-detector row CT (**c**). **e** Intraoperative photograph shows branches of the anterior cerebral artery adhering tightly to the tumor

Discussion

Imaging technology for identifying thinner vessels ultraselectively, for determining more complex vessel morphology, and for the accurate placement of surgical devices into the correct access points has become increasingly important in endovascular treatment. Clear visualization of vessels with sizes in the submillimeter range and the ability to check the results of treatment during a procedure can be obtained using high-quality Angio systems. We used the Allura Xper FD20/20 Angio system with XperCT functionality of rotational X-ray CBCT based on the high spatial resolution of 154 μm/pixel imaging technology. The use of low 80-kV exposure allowed even higher spatial resolution.

Two different image-processing algorithms are available in this Angio system, termed mode 1 and mode 2 in this study. Mode 1 was developed for stent visualization [8], while mode 2 was developed for vessel visualization [9]. Commercially, mode 2 is named VasoCT. Several studies have reported that imaging using 80-kV high-resolution XperCT with VasoCT is useful in endovascular treatment [10, 11], although the differences between the two modes have not been described. We found that mode 1 was superior in high-frequency spatial resolution, whereas mode 2 was superior in contrast resolutions with lower noise. We used the 80-kV high-resolution XperCT in both mode 1 and mode 2 properly. Further, optimized dilutions of contrast material provided good contrast images for enhanced anatomy of the soft tissues, vessels, and bones at the same time in a lesion. Mode 1 is typically used in cases in which the region of interest was inside of a bone or a contacting bone. Mode 2 has been used for visualizing weak contrast media or thin vessels. These selections are helpful at the planning phase of surgery, as they afford superior visualization of vessels and surrounding anatomy compared with CT and MR in localized disease.

When using 80-kV high-resolution XperCT with these modes, local anesthesia sedation control should be considered on a case-by-case basis, as there is a risk of movement artifact during the relatively long 20-s scan time. The small FOV for 80-kV high-resolution XperCT is not generally problematic when used for a localized targeted legion. Our new imaging technique is invasive compared with other modalities. However, when this technique is applied to appropriate cases, it is particularly useful for preoperative planning. We propose that the following three types of clinical uses are appropriate with this system.

Imaging of the distal dural ring and the surrounding structure of the cavernous sinus for paraclinoid aneurysms by 80-kV high-resolution XperCT with mode 1

When evaluating a potential paraclinoid carotid artery aneurysm before surgery, it is important to determine whether the aneurysm is inside or outside of the dura mater to determine the risk of subarachnoid hemorrhage as well as the surgical indications and prognosis. The juxta-dural ring area surrounded by a bony structure is a complex anatomical structure, for which the DDR is the most important anatomical landmark [12]. For image-based discrimination of a paraclinoid carotid artery aneurysm before surgery, the structure of the ophthalmic artery, the anterior clinoid process, the tuberculum sellae, and the optic strut can be used as anatomical landmarks [12–14].

The visualization approaches to the DDR by 3D-CTA and by MRI have been reported. For 3D-CTA, an imaging method that uses shaded surface reconstruction with anatomical data and volume rendering with adjustment of the threshold was described [15]. For MRI, imaging methods using the fusion of noncontrast and the contrast interference in steady state (CISS) method and MRA, contrasted 3D-MRA, and contrasted 3D-CISS have been reported. Additionally, studies of 3D-SPACE (sampling perfection with application-optimized contrast using different flip angle evolutions) sequences, T2 turbo-spin echo sequences, and noncontrasted 3D time-of-flight (TOF) by 3T MRI with high signal-to-noise (S/N) ratios have been conducted [16–20]. However, these imaging methods show the DDR indirectly. The DDR shown by these imaging modalities is a boundary structure of surrounding anatomy, based on contrast differences among the cavernous sinus, cerebrospinal fluid, internal carotid artery, and the aneurysm. We achieve this by adjusting the contrast dilution for direct visualization of the DDR, even in cases in which the aneurysm was surrounded by the bone. In the cases in which the aneurysm contacts the dura directly, since the contrast difference between the aneurysm and dura is less, further research regarding how to adjust the contrast may be necessary.

Imaging of thin blood vessels, especially the stream of the Sylvian vein and perforators, by 80-kV high-resolution XperCT with mode 2

The trans-Sylvian approach is a basic surgical approach widely used for aneurysms in the Wills ring and for parasellar tumors. Identifying the stream of the Sylvian vein is important to obtain a wider operational view with keeping veins on detaching frontal lobe or temporal lobe from the Sylvian fissure [21, 22]. Although approaches to detaching the Sylvian vein have been discussed (e.g., whether it should be performed via the frontal lobe or temporal lobe, or in-between), in practice, the approach is often determined during surgery. The inlet/outlet flow pattern and the approximate number of superficial Sylvian veins can be identified to some extent on normal DSA. However, for the planning phase of a surgery, the 80-kV high-resolution XperCT with mode 2 can show thinner veins compared with conventional DSA, as well as the details of the connecting portions of the veins in the operative view. Using 80-kV high-resolution XperCT with mode 2, the imaging of both arteries and veins is acquired together, although a one-by-one anatomical check is still necessary.

Although conventional 3D CT angiography can depict perforators to some extent, 80-kV high-resolution XperCT with mode 2 provides better visualization in cases that have smaller perforators and lack the density of contrast medium under the influence of laminar flow and turbulent flow, especially at the site of posterior circulation.

Imaging of a brain tumor and its surrounding anatomy showing detailed related locations by 80-kV high-resolution XperCT with mode 1 and mode 2

Conventional DSA is associated with a risk of neurological complications, and thus CT and MRI have tended to be used as an alternative in brain tumor surgery. The 80-kV high-resolution XperCT with mode 2, with its quite high spatial resolution and superior contrast resolution, can visualize thinner vessels such as feeders, drainers, and passing arteries, which are not observed using other normal imaging modalities. The 80-kV high-resolution XperCT with mode 1 provides better contrast in cases of skull base tumors surrounded with bone structure. Clear visualization of the structures, which are identified during the actual operation, can be obtained using these new imaging techniques properly based on the tumor locations.

Conclusion

Eighty-kilovolt high-resolution CBCT imaging combining an optimized protocol has the potential to provide detailed anatomical structure for neurosurgical operations when the most suitable modes and contrast protocols are utilized. When this imaging is applied to appropriate cases, it can provide new information on thinner vessels and anatomy, which are otherwise difficult to visualize with alternative modalities. Although anatomical confirmation of such images in the focused region is still required during surgery, 80-kV high-resolution CBCT can be particularly valuable for the presurgery planning phase.

Ethical standards and patient consent We declare that all human studies have been approved by the local Ethics Committee and have therefore been performed in accordance with the ethical standards laid down in the 1964 Declaration of Helsinki and its later amendments. Patient consent was waived for this retrospective study; however, CBCT studies were performed with informed consent of the patient or the patient's relatives.

Conflict of interest We declare that we have no conflict of interest.

References

1. Vertinsky AT, Schwartz NE, Fischbein NJ, Rosenberg J, Albers GW, Zaharchuk G (2008) Comparison of multidetector CT angiography and MR imaging of cervical artery dissection. AJNR Am J Neuroradiol 29:1753–1760. doi:10.3174/ajnr.A1189
2. Tomandl BF, Klotz E, Handschu R, Stemper B, Reinhardt F, Huk WJ, Eberhardt KE, Fateh-Moghadam S (2003) Comprehensive imaging of ischemic stroke with multisection CT. Radiographics 23:565–592. doi:10.1148/rg.233025036
3. Mnyusiwalla A, Aviv RI, Symons SP (2009) Radiation dose from multidetector row CT imaging for acute stroke. Neuroradiology 51: 635–640. doi:10.1007/s00234-009-0543-6
4. Miley JT, Taylor RA, Janardhan V, Tummala R, Lanzino G, Qureshi AI (2008) The value of computed tomography angiography in determining treatment allocation for aneurysmal subarachnoid hemorrhage. Neurocrit Care 9:300–306. doi:10.1007/s12028-008-9109-4
5. Akpek S, Brunner T, Benndorf G, Strother C (2005) Three-dimensional imaging and cone beam volume CT in C-arm angiography with flat panel detector. Diagn Interv Radiol 11:10–13
6. Mordasini P, Al-Senani F, Gralla J, Do D-D, Brekenfeld C, Schroth G (2009) The use of flat panel angioCT (DynaCT) for navigation through a deformed and fractured carotid stent. Neuroradiology 52: 629–632. doi:10.1007/s00234-009-0556-1
7. Soderman M, Babic D, Holmin S, Andersson T (2008) Brain imaging with a flat detector C-arm: technique and clinical interest of XperCT. Neuroradiology 50:863–868. doi:10.1007/s00234-008-0419-1
8. Patel NV, Gounis MJ, Wakhloo AK, Noordhoek N, Blijd J, Babic D, Takhtani D, Lee SK, Norbash A (2011) Contrast-enhanced angiographic cone-beam CT of cerebrovascular stents: experimental optimization and clinical application. AJNR Am J Neuroradiol 32:137–144. doi:10.3174/ajnr.A2239
9. Blanc R, Pistocchi S, Babic D, Bartolini B, Obadia M, Alamowitch S, Piotin M (2012) Intravenous flat-detector CT angiography in acute ischemic stroke management. Neuroradiology 54:383–391. doi:10.1007/s00234-011-0893-8
10. Caroff J, Mihalea C, Neki H, Ruijters D, Ikka L, Benachour N, Moret J, Spelle L (2014) Role of C-Arm VasoCT in the Use of endovascular WEB flow disruption in intracranial aneurysm treatment. AJNR Am J Neuroradiol. doi:10.3174/ajnr.A3860
11. Kizilkilic O, Kocer N, Metaxas GE, Babic D, Homan R, Islak C (2012) Utility of VasoCT in the treatment of intracranial aneurysm with flow-diverter stents. J Neurosurg 117:45–49. doi:10.3171/2012.4.jns111660
12. Oikawa S, Kyoshima K, Kobayashi S (1998) Surgical anatomy of the juxta-dural ring area. J Neurosurg 89:250–254. doi:10.3171/jns.1998.89.2.0250
13. Matsumura Y, Nagashima M (1999) Anatomical variations in the origin of the human ophthalmic artery with special reference to the cavernous sinus and surrounding meninges. Cells Tissues Organs 164:112–121
14. Hashimoto K, Nozaki K, Hashimoto N (2006) Optic strut as a radiographic landmark in evaluating neck location of a paraclinoid aneurysm. Neurosurgery 59:880–887. doi:10.1227/01.neu.0000232664.02190.e1
15. Murayama Y, Sakurama K, Satoh K, Nagahiro S (2001) Identification of the carotid artery dural ring by using three-dimensional computerized tomography angiography. Technical note. J Neurosurg 95:533–536. doi:10.3171/jns.2001.95.3.0533
16. Watanabe Y, Makidono A, Nakamura M, Saida Y (2011) 3D MR cisternography to identify distal dural rings: comparison of 3D-CISS and 3D-SPACE sequences. Magn Reson Med Sci 10:29–32
17. Watanabe Y, Nakazawa T, Yamada N, Higashi M, Hishikawa T, Miyamoto S, Naito H (2009) Identification of the distal dural ring with use of fusion images with 3D-MR cisternography and MR angiography: application to paraclinoid aneurysms. Am J Neuroradiol 30:845–850. doi:10.3174/ajnr.A1440
18. Tsuboi T, Tokunaga K, Shingo T, Itoh T, Mandai S, Kinugasa K, Date I (2007) Differentiation between intradural and extradural locations of juxta-dural ring aneurysms by using contrast-enhanced 3-dimensional time-of-flight magnetic resonance angiography. Surg Neurol 67:381–387. doi:10.1016/j.surneu.2006.08.006
19. Hirai T, Kai Y, Morioka M, Yano S, Kitajima M, Fukuoka H, Sasao A, Murakami R, Nakayama Y, Awai K, Toya R, Akter M, Korogi Y, Kuratsu J, Yamashita Y (2008) Differentiation between paraclinoid and cavernous sinus aneurysms with contrast-enhanced 3D constructive interference in steady- state MR imaging. Am J Neuroradiol 29: 130–133. doi:10.3174/ajnr.A0756
20. Thines L, Lee SK, Dehdashti AR, Agid R, Willinsky RA, Wallace CM, Terbrugge KG (2009) Direct imaging of the distal dural ring and paraclinoid internal carotid artery aneurysms with high-resolution T2 turbo-spin echo technique at 3-T magnetic resonance imaging. Neurosurgery 64:1059–1064. doi:10.1227/01.neu.0000343523.67272.34
21. Tanriover N, Rhoton AL Jr, Kawashima M, Ulm AJ, Yasuda A (2004) Microsurgical anatomy of the insula and the sylvian fissure. J Neurosurg 100:891–922. doi:10.3171/jns.2004.100.5.0891
22. Suzuki Y, Matsumoto K (2000) Variations of the superficial middle cerebral vein: classification using three-dimensional CT angiography. AJNR Am J Neuroradiol 21:932–938